A LEVEL-SET MASS-CONSERVATIVE MESH ADAPTATION TECHNIQUE FOR IN-FLIGHT ICE ACCRETION MULTI-STEP SIMULATIONS

Alessandro Donizetti[*†]**, Barbara Re**[†] **and Alberto Guardone**[†]

[†] Department of Aerospace Science and Technology
Politecnico di Milano
Via La Masa 34, 20156 Milano, Italy
e-mail: alessandro.donizetti@mail.polimi.it, barbara.re@polimi.it, alberto.guardone@polimi.it

Key words: Multi-step Ice Accretion, Level-Set Method, Unstructured Grids, Mass Conservation

Abstract. This paper presents an innovative approach to model evolving boundaries problems due to the accumulation or erosion of material over a surface, offering a robust alternative to standard algebraic methods. The strategy is based on the level-set method and it allows the local conservation of the prescribed mass material accounting for the curvature of the body. No partial differential equations are solved for the level-set function, but simple geometric quantities are used to provide an implicit discretization of the new updated boundary. The method is applied to body-fitted unstructured grids, that allow a good representation of arbitrarily complex geometries. Two multi-step in-flight ice accretion simulations over a NACA0012 are presented to show the feasibility and adaptability of the method, that can be also extended to three-dimensional applications.

1 INTRODUCTION

In-flight ice accretion is indeed a safety issue in aeronautics, since it leads to a significant degradation of the aerodynamic performances and aircraft handling. The analysis and design in these peculiar conditions call for ad-hoc CFD simulation tools, coupling the external aerodynamics, droplet trajectories, thermal systems and ice growth. A crucial aspect that characterizes and makes these simulations challenging is the formation, and evolution in time, of complex ice geometries, resulting from the ice accretion over the body surface and/or previously formed iced. Ice prediction softwares generally handle this aspect by means of a quasi-steady, sequential approach that, starting from accurate simulations of the flow field around the wing at a certain time t^n, predicts the trajectories of water droplets impacting the surface and determines the amount of ice that accretes over each boundary cell, be it a portion of the clean wing or of the already iced geometry,

during the time step $\Delta t = t^{n+1} - t^n$. At this point, to advance the simulation in time, the computational mesh must be updated to capture the position of the new interface between air and ice, resulting from ice accretion. The first steps of this procedure are not discussed in this paper, which, conversely, focuses on the mesh update step. From the CFD point of view, aerodynamic solvers usually require a body-fitted mesh, where the ice geometry plays the role of a rigid body, similar to the wing. Hence, in this context, capturing the new interface requires to move the mesh boundaries to precisely track the ice geometry resulting from the accumulation of the prescribed amount of ice during the time step Δt. One possibility is to use conservative a mesh displacement technique to displace the mesh [1] [2], although front collision might be difficult to detect.

In this work, we propose a novel strategy to adapt the mesh to the new air-ice interface that conserves locally the mass of ice to be added to the surface. Actually, we use the ice prediction as a framework to explain and validate the proposed methodology, which can be virtually adopted in diverse applications that require to deform a body-fitted mesh to conservatively account for the accumulation or erosion of a prescribed volume of material on the boundary. Examples may include the erosion of thermal protection material in re-entry flights and material deposition in additive manufacturing.

The accumulation or erosion of a material may generate complex interfaces that cannot be tracked by straightforward node displacement, which would result in element entanglement and mesh invalidation. In this work, we circumvent this problem by combining a level set formulation [3] with mesh adaptation techniques [4]. Moreover, we enforce a local correction of the prescribed boundary displacement (representing material accretion) according to the boundary curvature to locally conserve the amount of material.

Considering a single time-step, given as inputs the computational grid and the volume of the material that accumulates over each boundary edge along its normal direction, the key steps of the proposed strategy are:

1. piece-wise linear representation of the interface that enforces local conservation;

2. implicit definition of the interface through a level-set formulation, based on a signed distance field where the interface is defined by the 0-level;

3. mesh adaptation to accurately describe the interface;

4. extraction of the boundary discretization compliant with the updated position of the interface, to generate the new body-fitted mesh.

The last step leaves open the possibility of generating unstructured, structured, or hybrid meshes for the fluid domain.

In this paper, we illustrate the conservative, adaptive, level-set based, interface tracking strategy over two-dimensional unstructured grids and we validate it through multi-step simulations of ice accretion around airfoils, where the grid is adapted to the new ice shape at every time step. To this purpose, we have integrated the proposed strategy

into PoliMIce [5], the computational suite for in-flight ice accretion problems under development at Politecnico di Milano. Since a Navier-Stokes solver is used to compute the aerodynamic field, hybrid body-fitted meshes are generated from the interface-compliant boundary discretization with the software uhMesh [6].

The idea to represent the air-ice interface through a level-set function was already proposed in [7] and [8]. The novel aspects of this work are the following ones. First, according to our knowledge, this is the first time the issue of material conservation is addressed in the context. Second, thanks to mesh adaptation, our approach is able to deal with complex geometries, which could otherwise jeopardize the advancement of ice-accretion simulations that update the mesh by simple boundary node displacement. Finally, as stated before, the strategy is not limited to ice accretion, but it can be applied also to any context that requires to deal with the accretion or erosion of a material over a boundary of a body-fitted mesh. Indeed, we do not solve an advection equation for the level set function, but we simply combine two sets of information—the amount of material to be accreted at the boundary and the distance of each grid node from the boundary—to define the new boundary discretization.

2 METHODOLOGY

In this section, we describe the locally conservative, level-set, interface tracking strategy developed in our work. Hereinafter, we refer only to accumulation (or accretion) of the material (with ice occasionally brought as an example), but the same concepts can be smoothly extended also to erosion or material ablation. First, we describe in sec. 2.1 how we define and discretize the interface under the level set formulation, starting from a given distribution of the material on the boundary. Then, in sec. 2.2, we detail how we compute a piecewise linear distribution of the thickness that enforces local material conservation. Finally, we highlight some remarks about the whole procedure in sec. 2.3.

2.1 Implicit interface discretization under the level set formulation

The level-set method is a general framework for the computation of curves and surfaces using an implicit formulation [3]. Given a 2D domain $\Omega \subset \mathbb{R}^2$, a curve can be represented by the 0-level set of the auxiliary function $\phi(\mathbf{x}, t)$, with $\mathbf{x} \in \Omega$. Considering the accretion of a material over the boundary of the computational domain otherwise filled with air, $\phi(\mathbf{x}, t)$ is a signed distance function defined so that

- $\phi(\mathbf{x}, t) < 0$ in the portion of the domain occupied by material,

- $\phi(\mathbf{x}, t) > 0$ in the portion of the domain not occupied by material (air for in-flight ice accretion),

- $\phi(\mathbf{x}, t) = 0$ interface.

Standard level set approaches compute the evolution of the quantity $\phi(\mathbf{x}, t)$ by solving a Cauchy problem for the advection equation associated with the accretion velocity [3].
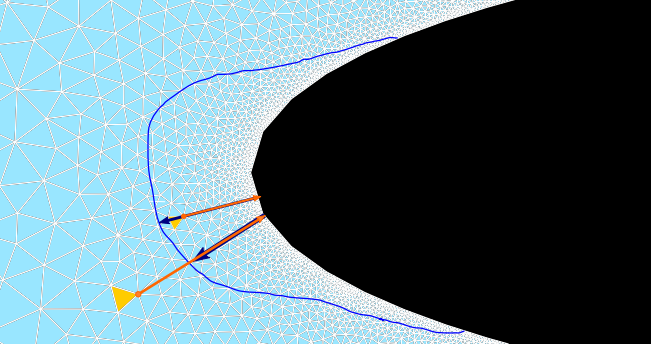
Figure 1: The orange arrows represent the exact distance of two generic points from the solid boundary ($d_i = \|\mathbf{x}_i - \mathbf{x}_{i|B}\|$), while the blue ones indicate the prescribed material thickness on the corresponding cells ($B(\mathbf{x}_{i|B})$).
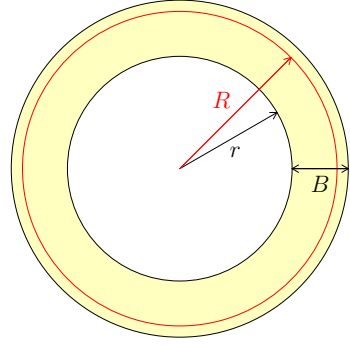
Figure 2: Accretion of mass m over a circle of radius r. B is the computed thickness that does not allow mass conservation, while R is the final radius that allows the conservation of the prescribed mass m.

In contrast, in this work, we directly build a discrete field that provides an implicit definition of the interface location, for the time considered. At each grid point i, we define the quantity $\phi_i = \phi(\mathbf{x}_i)$ as

$$\phi_i = d_i - B_i\,, \qquad \text{with} \quad d_i = \left\|\mathbf{x}_i - \mathbf{x}_{i|B}\right\| \;\; \text{and} \;\; B_i = B(\mathbf{x}_{i|B}), \tag{1}$$

where $\mathbf{x}_{i|B}$ is the point on the solid boundary closest to $\mathbf{x}_i$, d_i is the distance of the point i from $\mathbf{x}_{i|B}$, and B_i is the prescribed amount of material for the point $\mathbf{x}_{i|B}$. We detail how to compute this value starting from a piece-wise constant material distribution in section 2.2. See fig. 1 for an illustration.

On triangular meshes of interest here, the definition of the level-set value at the each node of the mesh provides a piecewise linear approximation of the function $\phi(\mathbf{x})$ over the domain Ω. Hence, to extract the interface requires to extract the discretization of the 0-level set of $\phi(\mathbf{x})$. To accomplish this task, we use the open-source libmmg2d library [4, 9], which performs two steps: domain splitting and mesh improvement. First, for each element crossed by the 0-level set, the edges intersected by the 0-level set are split, by adding a new point at the intersection between the 0-level curve and the edge. Then, quality-oriented mesh adaptation techniques are used to improve the accuracy of the curve discretization. At this point, we can extract individually each part of the domain (for instance, in ice accretion problems, the part of the mesh with negative ϕ can be used to investigate heat transfer properties or ice cracking patterns), as well as the set of edges connecting all points at $\phi = 0$ which represents the target air-material interface at the new time step.

2.2 Local correction for mass conservation

A crucial aspect while simulating material accumulation is the conservation of material mass, which, considering a constant density material, directly correlates to area conserva-

tion. In this context, loss or gain of material mass can arise at different levels: during the extraction of points in the level-set formulation, during the new mesh generation process, or during the air-material tracking. While the first and the second causes are strongly related to grid spacing, and can be alleviated by smaller grid elements around the body, the third one is a much more delicate aspect, correlated to the body geometry, that we address in this work.

To clarify the issue under investigation, consider a circle of radius r, subjected to a constant material accretion rate, as shown in fig. 2. Suppose that a certain mass of material m is distributed uniformly over the circle. The simplest approach is to impose on each cell a constant thickness $B = m/(\rho L_r)$, with L_r the circumference of the inner circle. If doing so, the added material amounts to the area of the circular crown of outer radius $r + B$ and inner radius r, that is

$$A_{added} = \pi((r + B)^2 - r^2) \,.$$

However, if we consider that the circle is perfectly discretized and its length is equal to the circumference, the real area we should add is equal to

$$A_{real} = 2\pi r B \,.$$

Therefore, we should assign a different value R to the external circumference, imposing the conservation of the desired area. The difference between the mass conservative radius R and the one obtained by simply adding the thickness B to radius of the clean geometry depends, in a non linear way, only on the ratio B/r. In particular, the larger this ratio, the greater is the mass error introduced if no correction is applied.

Note that the conservation problem outline above does not stem from the discretization of the circle, but from the fact that its boundary is curved. Indeed, both the constant thickness approach and the conservative mass approach yield to the same results if the surface is perfectly linear, such as a flat plate. The same issue occurs when we have to accumulate a certain mass (or area) of material over two consecutive, non-planar cells. If we compute the cell thickness corresponding to a uniform distribution over the length of the two cells and propagate it perpendicularly to each cell, two things may occur: if the surface is convex, a gap is created at the vertex P; if the surface is concave, the two layers overlap, as shown in fig. 3. Now, if we model the new interface as the continuous broken line connecting the updated positions (A', P'_1, P'_2, and B' in fig. 3), the convex and concave conditions result, respectively, in a gain and in a loss of the accumulated mass with respect to theoretical one.

To conserve the material mass, we need to the take into account the real shape obtained after thickness propagation when we define the level-set function $\phi(\mathbf{x})$ according to eq. (1). Hence, we need to correct the assigned thickness value, so that the final material mass will be equal to prescribed one. More precisely, we compute a new piecewise linear distribution of the thickness $\widetilde{B}(\mathbf{x}_b)$, starting from corrected node values. While defining these corrected
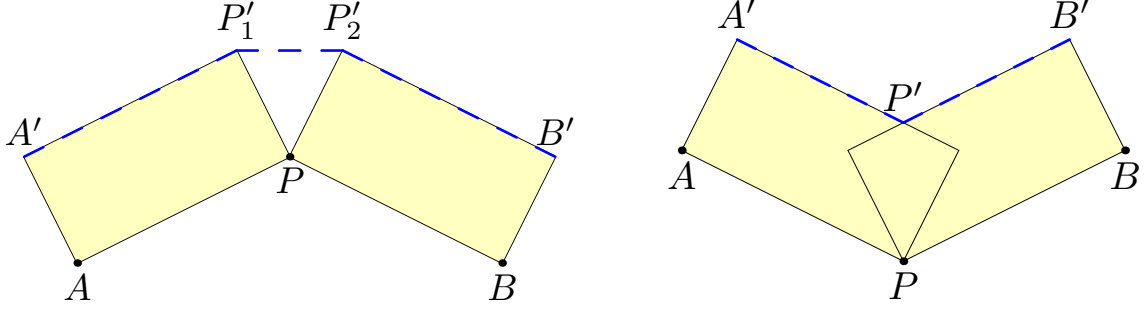
Figure 3: Schematic representation of the gain (left) and loss (right) of material due to the presence of curved, discretized, geometries.
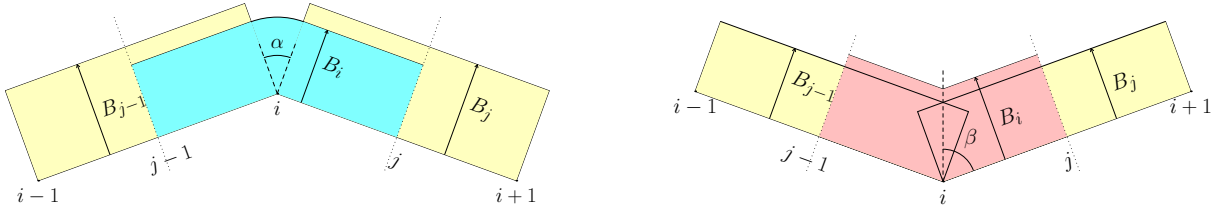

Figure 4: Local correction of the assigned thickness to a generic node for the convex (left) and concave case (right). Index i is used for nodes, while index j is used for edges.

node values, we impose to locally conserve an amount of mass A_i equivalent to the sum of half of the masses prescribed on the adjacent cells.

Figure 4 displays the definition of the corrected thickness at the boundary point i, for the convex and the concave case. In the former, once a value is assigned at the node, since the distance value is not associated to any directional information, all the grid points within the circular sector of radius equal to the prescribed ice thickness $\widetilde{B}_i$ and angle α, having as nearest neighbor the vertex node i, will have a negative value of the level-set function ϕ. To compute the value of $\widetilde{B}_i$, we express analytically the resulting area (blue one in fig. 4) as function of the unknown thickness $\widetilde{B}_i$. By setting this area equal to the area A_i, we can compute the correct node value $\widetilde{B}_i$ that guarantees the local conservation of the mass prescribed on the adjacent cells. In the concave case no gaps are formed, but we have instead a loss of area. To compensate it, we assign an increased thickness $\widetilde{B}_i$ at the node, keeping the sides of the resulting polygon (the short basis of the two trapezoids forming the red area in fig. 4) parallel to the walls. To locally conserve mass, we impose that the sum of the red areas is equal to A_i.

2.3 Conservative level-set based, interface tracking strategy

In sec. 2.2, we have discusses the conservative correction for a single boundary node. When the correction is applied to the whole mesh, the resulting geometry is slightly different from the ones depicted in Fig. 4. Unless we have a constant ice accretion rate
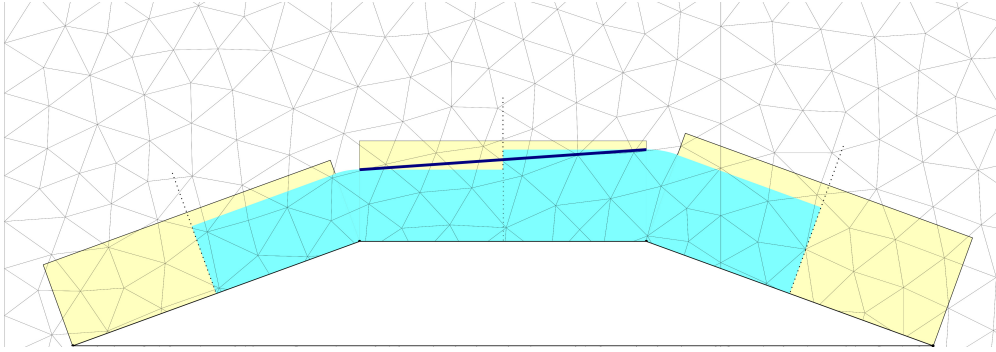
Figure 5: The area corresponding to the original prescribed thickness over each edge is represented in yellow. The blue area corresponds to the local modified thickness. The dark blue line is the actual shape that we are defining by means of the linear interpolation of the values assigned to the edge's delimiting nodes. In particular, the mesh adaptation strategy will cut the mesh exactly along this line.

on a surface with constant curvature, every point of the boundary mesh will have, after the angle-dependent correction, a different value of $\widetilde{B}_i$. When we compute the implicit function ϕ_i at a generic grid point i, the material thickness value $\widetilde{B}_i$ is the result of the linear interpolation of the nodal values $\widetilde{B}_i$ at the boundary point closest to i, thus (1) is replaced by

$$\phi_i = d_i - \Pi_{\tilde{B}}(\mathbf{x}_{i|B}), \tag{2}$$

where d_i and $\mathbf{x}_{i|B}$ are the same as in (1), and $\Pi_{\tilde{B}}(\mathbf{x}_B)$ is the piecewise linear interpolation operator of the corrected thickness $\widetilde{B}$ over the boundary. An example of a possible resulting shape using the level-set function (2) is depicted in fig. 5.

It is important to highlight that the proposed strategy is only locally conservative. When considering more than two adjacent cells originating a convex-concave combination, the true mass added, according to the interpolated thickness, does not equate to the sum of the original mass prescribed on each cell. We could recover the exact mass conservation by adding a control point at the medium point of the cell and prescribing a new thickness value taking into account the final interpolation, however we avoid this further complexity since the introduced error is negligible if the prescribed original thickness is not too big with respect to the cells length.

An additional potential source of error stems from large concave angles between adjacent boundary edges, which would cause a significant loss of mass due to the overlapping. The correction described in sec. 2.2 could transform the initial concavity into a spike. However, adding so much material to complex geometries in a unique step is not recommended, as the whole geometry would change during the accretion process, leading to very different final geometries and, hence, inaccuracies.

Table 1: Error between the constant thickness and mass conservative approach, computed analytically.

	1 step	2 steps	4 steps	8 steps
Relative error, $|A_{added} - A_{real}|/A_{real}$	50%	18%	7.8%	3.6%
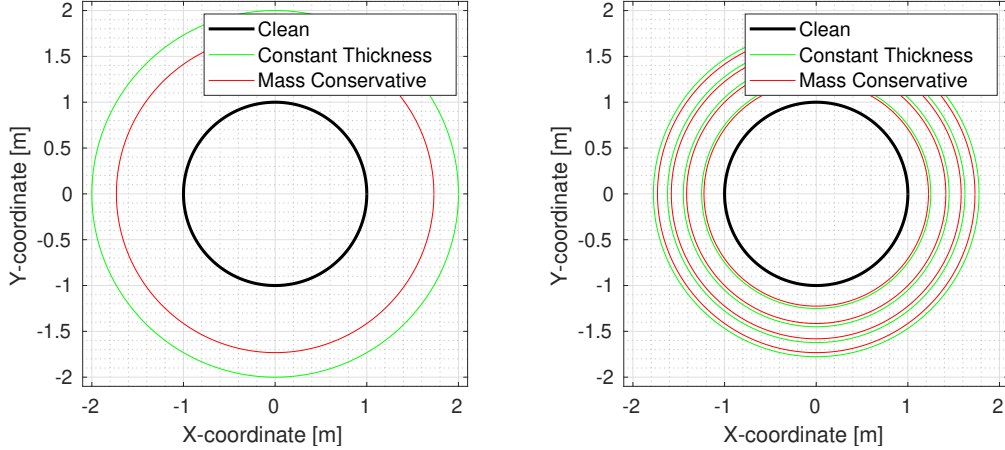
Figure 6: Representation of the intermediate thicknesses relative to an accretion of a mass $m = 2$ kg/s $\cdot$ 1000 s, obtained subdividing the total mass m in a single step (left) and in 4 steps (right). The density of the material is 1000 kg/m^2 For each step we display the constant thickness approach and the mass conservative one.

3 METHOD VERIFICATION

3.1 Uniform accretion over a circle

The first verification test is the uniform material accretion over a circle with unit radius at a constant rate of 2π kg/s. The final time of the simulation is 1000 s. Before applying the level-set formulation, we investigate analytically this problem. If we subdivide the total accretion time in substeps, as the mass accretes and the circle enlarges, the width of each circular crown shrinks. As a consequence, since the ratio B/r decreases over time, the error introduced by considering constant thickness instead of mass conservative thickness is reduced. The number of sub-steps has a huge impact on the final mass error, as illustrated by Fig. 6, which displays the resulting circles considering 1 and 4 sub-steps, with and without the local thickness correction for mass conservation. Table 1 reports the value of the mass error, defined as the relative difference between the resulting areas with and without thickness correction, performing 1, 2, 4, and 8 sub-steps.

Now, we apply the proposed conservative, level-set based, interface tracking strategy, considering again 1, 2, 4, and 8 sub-steps. In all cases, the error with respect to the area computed analytically is well below 1%, as reported in table 2. Figure 7 compares the extracted boundary nodes given by the level-set discretization of the interface with the ones given by analytical mass conservative curve, performing 1 and 4 sub-steps. At each sub-step, the interface is well captured by the proposed approach.

Table 2: Error between the analytical mass conservative approach and the level-set interface tracking.

	1 step	2 steps	4 steps	8 steps
Relative error, $|A_{l.s.} - A_{real}|/A_{real}$	0.03%	0.07%	0.19%	0.16%
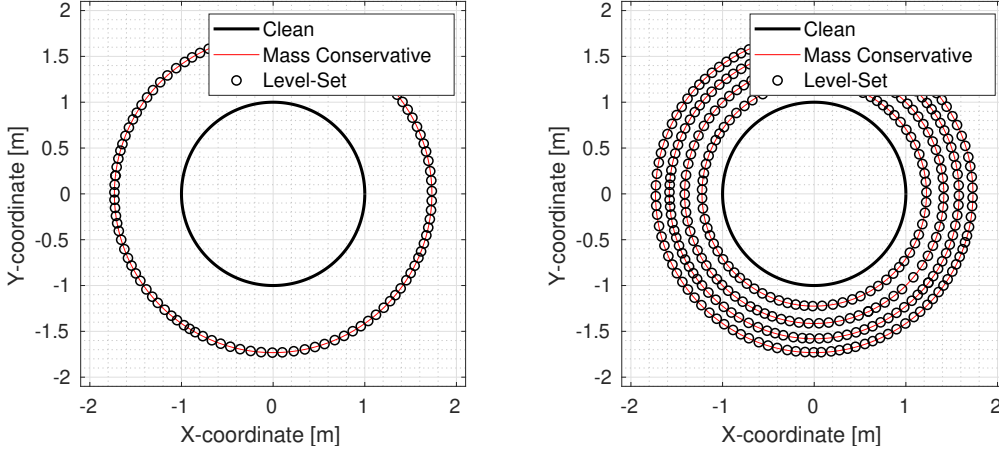
Figure 7: Representation of the intermediate thicknesses relative to an accretion of a mass m, obtained subdividing the total mass in a single step (left) and in 4 steps (right). For each step is represented the thickness obtained with level-set method and the theoretical mass conservative one. Regarding the first one, we represented the points that actually constitute the interface within Mmg.

3.2 Uniformly distributed accretion over an ellipse

We consider now the accretion of a given mass m, over an ellipse of semi-axes $a = 6$ m and $b = 2$ m. Differently from the previous test, the curvature is not constant. Figure 8 displays the interfaces computed by means of the level-set based interface tracking assuming a constant thickness $B = m/(\rho L_e)$, with L_e the perimeter of the ellipse, and imposing the local thickness correction that conserves the given mass m. The mass error (with respect to the analytical value) with the local correction is 0.05%, while it is 11.76% without correction. Moreover, it is evident that, where the curvature is bigger, the correction is much more important. In terms of thickness, at the point of maximum curvature, the mass preserving thickness is only 66% of the constant thickness B.

4 ICING SIMULATIONS

In this section, we present two ice-accretion problems over a NACA0012 airfoil, representative of two different icing phenomena, that is, glaze and mixed ice [10]. We can compare the results of the proposed conservative level-set interface tracking strategy to the available numerical [8] and experimental [11] data. Test conditions are reported in
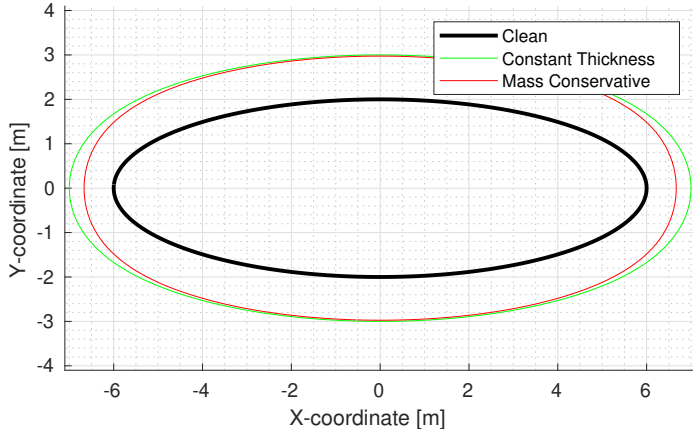
9

Figure 8: Accretion of a uniformly distributed mass over a discretized ellipse. The constant thickness displacement is represented in green, while the mass conservative thickness is represented in red.

Table 3: Test conditions: input to the problem are the angle of attack, the freestream velocity, temperature and pressure, the liquid water content (LWC) of the cloud, i.e. the grams of water contained in a cubic meter of air, the droplet median volume diameter (MVD) and the total icing exposure time.

Test	AoA	Velocity	Temperature	Pressure	LWC	MVD	Icing Time
	[°]	[m/s]	[K]	[kPa]	[g/m^3]	[μm]	[s]
Glaze ice	4.0	58.10	266.3	95.61	1.30	20	480
Mixed ice	4.0	93.89	260.8	92.06	1.05	20	372

table 3. To assess convergence, we use different numbers of steps [1] and different mesh discretization parameters are used. In particular we characterize each mesh by the minimal boundary edge size h_e.

4.1 Glaze Ice

This glaze ice condition are characterized by a relatively high temperature, which allows water run-back after the droplets impinging point. Figure 9 shows the results obtained in three simulations: performing 10 steps over a medium grid ($h_e = 0.001$ m), 30 steps over the same medium grid, and 30 steps over a fine grid ($h_e = 0.0005$ m). The three simulations suggest a convergence of the ice shape, especially in the lower airfoil surface, while in upper surface, the final geometry is strongly influenced by the first layers. Indeed, with larger elements and less layers, the angle ice forms with the airfoil is steeper than other cases. However, our results, especially on the lower surface, do not fit precisely experimental data, probably because the water run-back behavior is not well captured by the used model, which, instead, predicts the formation of a secondary horn.

---

[1]A single step includes one aerodynamic simulation, followed by the prediction of the droplet trajectory and of ice mass to be accreted.
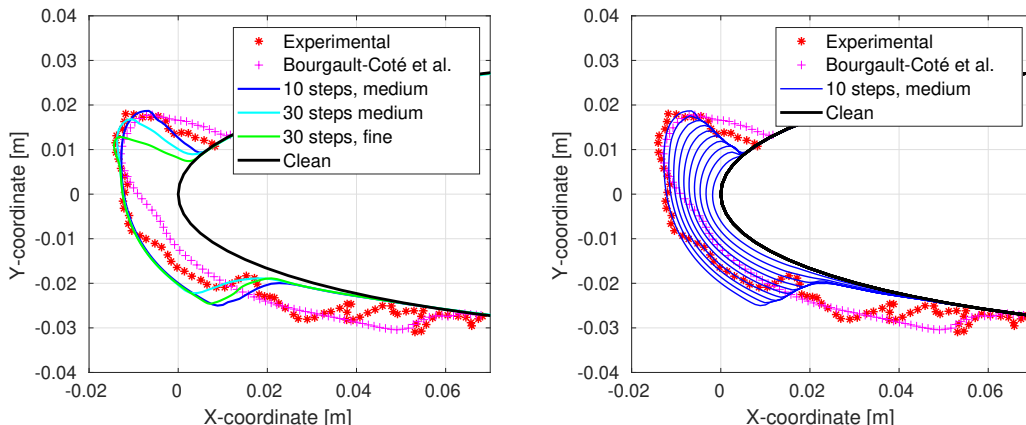
10

Figure 9: Glaze Ice on a NACA0012 airfoil. Comparison of the final results obtained with different numbers of steps and with different discretizations of the surface mesh (left) and intermediate layers for the 10 steps simulation over the medium grid (right).

4.2 Mixed Ice

The mixed ice case is characterized again by runback water, but only in the stagnation point region. Figure 10 shows the results obtained in three simulations: performing 20 steps over a coarse grid ($h_e = 0.001$ m), 37 steps over the medium grid ($h_e = 0.0005$ m), and 37 steps over a fine grid ($h_e = 0.0004$ m). The results leads to observations similar to ones made for the glaze ice test case, especially about the dependence, for the upper airfoil surface, on the size of the mesh elements, and the formation of a second small horn on the lower surface, which prevents the formation of a thicker layer.

5 CONCLUSIONS

We have proposed a new level-set based strategy to accurately track the interface implicitly defined by a discrete signed-distance field over an unstructured mesh. The proposed method is well-suited to simulation involving the accumulation of a material over some boundary of the computational domain. Among the notable features, this strategy is able to locally conserve the prescribed amount of material to be accreted over the boundary and to precisely track arbitrarily complex interfaces thanks to mesh adaptation. Although conceived and validated in the context of ice accretion over aerodynamic surfaces, the proposed strategy is standalone and it could be successfully exploited in different applications. Currently, we are working on the three-dimensional extension of this procedure and to its generalization over structured and hybrid grids.

REFERENCES

[1] B. Re, C. Dobrzynski, and A. Guardone. An interpolation-free ale scheme for unsteady inviscid flows computations with large boundary displacements over three-dimensional adaptive grids. *J. Comput. Phys.*, 340:26–54, 2017.
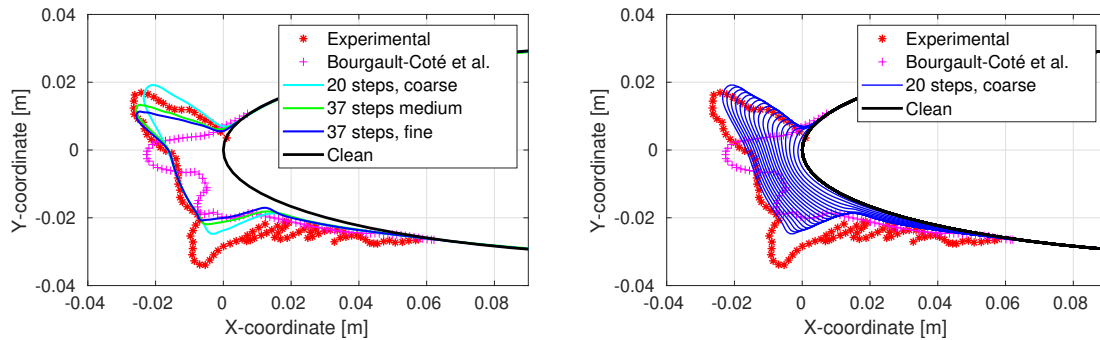
Figure 10: Mixed Ice on a NACA0012 airfoil. Comparison of the final results obtained with different numbers of steps and with different discretizations of the surface mesh (left) and intermediate layers for the 20 steps simulation over the coarse grid (right).

[2] L. Cirrottola, M. Ricchiuto, A. Froehly, B. Re, A. Guardone, and G. Quaranta. Adaptive deformation of 3d unstructured meshes with curved body fitted boundaries with application to unsteady compressible flows. *J. Comput. Phys.*, 433:110177, 2021.

[3] S. Osher and R. Fedkiw. *Level set methods and dynamic implicit surfaces*. Springer Science & Business Media, 2006.

[4] C. Dapogny, C. Dobrzynski, and P. Frey. Three-dimensional adaptive domain remeshing, implicit domain meshing, and applications to free and moving boundary problems. *J. Comput. Phys.*, 262:358–378, 2014.

[5] G. Gori, M. Zocca, M. Garabelli, A. Guardone, and G. Quaranta. Polimice: A simulation framework for three-dimensional ice accretion. *Appl. Math. Comput.*, 267:96–107, 2015.

[6] D. Dussin, M. Fossati, A. Guardone, and L. Vigevano. Hybrid grid generation for two-dimensional high-reynolds flows. *Computers & fluids*, 38(10):1863–1875, 2009.

[7] D. Pena, Y. Hoarau, and E. Laurendeau. A single step ice accretion model using Level-Set method. *J. Fluids Struct.*, 65:278–294, aug 2016.

[8] S. Bourgault-Cote, J. Docampo-Sánchez, and E. Laurendeau. Multi-Layer Ice Accretion Simulations Using a Level-Set Method With B-Spline Representation. In *2018 AIAA Aerosp. Sci. Meet.* American Institute of Aeronautics and Astronautics, 2018.

[9] C. Dapogny, C. Dobrzynski, P. Frey, and A. Froehly. Mmg PLATFORM. `www.mmgtools.org`.

[10] R.W. Gent, N.P. Dart, and J.T. Cansdale. Aircraft icing. *Philosophical Transactions of the Royal Society A: Mathematical, Physical and Engineering Sciences*, 358(1776):2873–2911, 2000.

[11] W.B. Wright, R.W. Gent, and D. Guffond. DRA/NASA/ONERA collaboration on icing research. Part 2; Prediction of airfoil ice accretion. (CR–202349), 1997.